The transition between undiluted and oligomer-diluted states of nearly monodisperse polystyrenes in extensional flow

Huang, Qian; Rasmussen, Henrik K.

Published in:
Rheologica Acta

Link to article, DOI:
10.1007/s00397-017-1032-1

Publication date:
2017

Document Version
Peer reviewed version

The transition between undiluted and oligomer diluted states of nearly monodisperse polystyrenes in extensional flow

Qian Huang[1], Henrik Koblitz Rasmussen[2]
(1) Department of Chemical and Biochemical Engineering,
(2) Department of Mechanical Engineering
Technical University of Denmark, DK-2800 Kgs. Lyngby, Denmark

Abstract

We have measured the startup and steady extensional viscosity of two narrow molar mass distributed (NMMD) polystyrenes, a 910 kg/mole and a 545 kg/mole, diluted in a NMMD 4.29 kg/mole styrene oligomer, with a wide concentration range from 90% down to 17%. The constant interchain pressure model, proposed by Rasmussen and Huang (2014) [1], predicts the extensional viscosity well for the dilutions with lower concentrations. However, for the 70% and 90% 545 kg/mole samples which represent the transition between the diluted and undiluted states, the model predictions are less satisfactory. Another concept based on interchain pressure, proposed by Wagner (2014) [2], also shows agreement with the measured data.

1 Introduction

In recent years, experiments on extensional viscosity of oligomer diluted narrow molar mass distributed (NMMD) polystyrene (Huang et al. 2013a; 2013b; 2015) [3, 4, 5] and poly methyl methacrylate polymers (Wingstrand et al. 2015) [6] have been reported. The oligomers used were all below the entanglement molecular weight, differentiating these blends from bidisperse blends in general. The oligomers, short enough to be in a random configuration in the rubbery state, were expected to be the most ideal solvents.

These studies were conducted to bridge the gap between the extensional flow measurements on NMMD polystyrene solutions (Bhattacharjee et al. 2002) [7] and polystyrene melts (Bach et al. 2003) [8]. The latter studies by Bhattacharjee et al. (2002) [7] and Bach et al. (2003) [8] showed the lack of universality with entanglement numbers in the flow dynamics of entangled polymer systems. The original work by Huang et al. 2013a [3], with systems containing the same entanglement number, also showed that the extensional viscosity of oligomer diluted polystyrene systems differed from other polystyrene solutions as long as the oligomer length was at least two Kuhn steps (Rasmussen and Huang 2014) [9]. As expected it differed from the extensional viscosity of undiluted melts as well. Solutions, included the one with short oligomer diluents, show the highest degree of strain hardening in extension, melt the lowest one and blends with long oligomers were inbetween (Rasmussen and Huang 2014) [9]. The studies in Huang et al. (2013a; 2013b) [3, 4] and Wingstrand et al. (2015) [6] were in a relatively narrow region of concentration ($45\% - 70\%$). The most recent study by Huang et al. (2015) [5] expanded the measurements on oligomer diluted NMMD polystyrenes with lower concentrations from 52% down to 13%.

Keeping the above efforts in mind, the first measurements of the extensional viscosity on NMMD polymer systems were actually published in the mid-seventies by Vinogradov and co-workers (Vinogradov et al. 1975) [10] who measured the startup of extensional stress of NMMD polyisoprenes.

However, the strain values that they reached were about 2, limiting the theoretical importance of their work. NMMD Polystyrenes are the best characterized polymer melts in extensional flow, but are not the only ones. As mentioned previously, Vinogradov and co-workers (Vinogradov et al. 1975) [10] measured NMMD polyisoprene in extensional flow in the seventies. In the recent years papers presenting measurements of extensional viscosity of NMMD polyisoprenes at high strain values have been published (Nielsen et al. 2009; Liu et al. 2013; Sridhar et al. 2014) [43, 44, 45]. Further Sridhar et al. (2014) [45] characterized a NMMD poly(n-butyl acrylate) in extension and most recently Alvarez (2016) [46] presented poly(methyl methacrylate) and poly(tert-butylstyrene) extensional measurements.

Looking at the constitutive models intended to capture the fluid mechanics of entangled monodisperse polymer systems in general, two recent ideas have appeared, concerning interchain pressure (Wagner 2014) [2] and monomeric friction (Yaoita et al. 2012; Iannirubertо at al 2012) [11, 12], respectively. In the models concerning monomeric friction reduction, the changeable functions (Masubuchi et al. 2014) [13] and parameters (Iannirubertо 2015; Park and Iannirubertо 2017) [14, 15] seem adequate to model the flow of all monodisperse polymer systems (Sridhar et al. 2014) [16]. Here we use the concept of interchain pressure to study monodisperse polymer systems with a wide concentration range from 90% down to 17%, and look at the transition between the diluted and undiluted states.

2 Materials and characterization

2.1 Materials

In this work we investigate the extensional viscosity of two NMMD polystyrenes at different concentrations. A 545 kg/mole polystyrene was diluted in a styrene oligomer with weight fraction of the polymer from 90% down to 28%, and another 910 kg/mole polystyrene was diluted to 17%.

The two polystyrenes used here are the same ones as used in Huang et al. (2013a; 2015) [3, 5]. They have weight based average molecular weight, M_w, of 545 kg/mole (PS545k) (Huang et al. 2013a) [3] and 910 kg/mole (PS910k) (Huang et al. 2015) [5] with polydispersity index, $PDI = M_w/M_n$, of 1.12 and 1.16 respectively. M_n is the mole based average molecular weight. The styrene oligomer is the same one as used in Huang et al. (2015) [5] with $M_w = 4.29$ kg/mole and $PDI = 1.04$.

All the samples were prepared using the procedure described by Huang et al. (2013a) [3] where the concentrations were verified by the peak areas of the bimodal curve in size exclusion chromatography. The styrene oligomer diluent is considerable shorter than the entanglement molecular weight of polystyrene but contains 7 Kuhn steps. The weight fraction of the polystyrenes in the oligomer dilution, θ, for the four prepared samples is listed in Table 1. Glass transition temperature T_g was measured by the differential scanning calorimetry (DSC) and the values are listed in Table 1 as well. Another three samples from literature are also listed in the table for the purpose of comparison.

2.2 Mechanical spectroscopy

The mechanical spectroscopy data were obtained from small amplitude oscillatory shear flow measurements using the ARES-G2 rheometer from TA Instruments. An 8 mm plate-plate geometry was applied with the samples staying under nitrogen. All the measurements were time-temperature superpositioned to 130°C.

To quantify the linear viscoelastic measurements, the BSW (Baumgaertel, Schausberg and Winter) (Baumgaertel and Winter 1992; Baumgaertel at al. 1990) [17, 18] formulation is used here for

the memory function. It is given as

$$M(t-t') = \int_0^\infty \frac{H(\tau)}{\tau^2} e^{(-(t-t')/\tau)} d\tau, \tag{1}$$

$$H(\tau) = n_e G_N^0 \left[\left(\frac{\tau}{\tau_{max}} \right)^{n_e} + \left(\frac{\tau}{\tau_c} \right)^{-n_g} \right] h(1-\tau/\tau_{max}) \tag{2}$$

where $h(x)$ is the Heaviside step function, G_N^0 is the plateau modulus, τ_{max} is the maximal relaxation time and τ_c is the largest relaxation time of the glassy modes. As in Rasmussen and Huang (2014) [1], the values of $n_e = 0.2$ and $n_g = 0.7$ are kept constant for the polystyrene samples. Further the plateau modulus scales theoretical ideal as $G_{N,\theta}^0 = \theta^2 \cdot 250 \cdot T/(403.15K)$ kPa (Rasmussen and Huang 2014 [1]), referred to 130°C as the reference temperature for the polystyrene samples. Notice this leaves τ_{max} and τ_c as the fitting parameters.

Some of the needed BSW parameters have been determined previously (Rasmussen and Huang 2014) [1] where the remaining values are calculated by fitting the mechanical spectroscopic data to the BSW model using the method from Rasmussen et al. (2000) [19]. The mechanical spectroscopic measurements with the corresponding BSW fittings are shown in Figure 1 and 2. The actual values of the parameters can be found in Table 1. For later use, the zero shear viscosity, η_0, is calculated as

$$\eta_0 = \int_0^\infty G(s)ds = n_e G_N^0 \tau_{max} \left(\frac{1}{1+n_e} + \frac{1}{1-n_g} \left(\frac{\tau_c}{\tau_{max}} \right)^{n_g} \right) \approx \frac{n_e}{1+n_e} G_N^0 \tau_{max} \tag{3}$$

based on the BSW parameters.

2.3 Extensional Measurements

The extensional measurements were performed using a filament stretching rheometer (FSR) as in Bach et al. (2003a;2003b) [8, 20]. More details of the FSR can be found in Marin et al. (2013) [21]. Experimentally the polystyrene samples were molded into cylindrical shaped samples with an initial diameter of D_i and an initial length of L_i. $D(t)$ is the central diameter of the sample during extension at time t. In the FSR the samples are commonly pre-stretched, with a rate considerably slower than the inverse largest relaxation time, to a central diameter of D_0. The extensional strain, known as the Hencky strain, is calculated as $\epsilon(t) = -2\ln(D(t)/D_0)$. During extension the start up of extensional viscosity, $\bar{\eta}^+$, is defined as

$$\bar{\eta}^+ = \frac{\sigma_{zz} - \sigma_{rr}}{\dot{\epsilon}_0}, \tag{4}$$

where the extensional stress is the difference between the axial, σ_{zz}, and radial, σ_{rr}, component of the stress tensor, $\boldsymbol{\sigma}$. A constant extensional rate, $\dot{\epsilon}_0$, is ensured during extension. The extensional rate is defined as $\dot{\epsilon} = d\epsilon/dt$. Before the initiation of the stretch (at $t = 0$) the material is stress free and at rest.

At small values of the Hencky strain, pre-strain ($2\ln(D_\mathrm{i}/D_0)$) and aspect ratio ($A_\mathrm{i} = 2L_\mathrm{i}/D_\mathrm{i}$), a shear contribution may add to the measured extensional force. Using the correction formula from Rasmussen et al. (2010) [22]

$$\sigma_{zz} - \sigma_{rr} = \frac{F(t) + m_f g/2}{\pi D(t)^2/4} \cdot \frac{1}{1 + (D(t)/D_\mathrm{i})^{10/3} \cdot \exp(-A_\mathrm{i}^3)/(3A_\mathrm{i}^2)}, \tag{5}$$

the initial extensional stress deviates less than 3% from the theoretically correct one. In equation (5) m_f is the weight of the sample and g is the gravitational acceleration (Szabo 1997) [23]. Notice that the assumption of uniform extension in the radial direction at the center of the sample has been estimated to be correct within a few percent (Nielsen et al. 2008) [24].

Table 1: Composition and linear viscoelastic parameters of the NMMD polystyrene systems at 130°C. The parameters for PS545k and $\theta = 0.525$ PS545k are taken from Rasmussen and Huang (2014) [1], and for $\theta = 0.33$ PS910k are taken from Rasmussen and Huang (2017) [26]. The parameters for the rest of the samples are obtained by fitting the relevant parameters from mechanical spectroscopical measurements, shown in Figure 1 and 2, to the BSW model (2) using the method from Rasmussen et al. (2000) [19]. The values of $n_e = 0.2$ and $n_g = 0.7$ are used for all the samples. θ is the weight fraction of the long polymer chain in the dilution. The diluent is the 4.29 kg/mole styrene oligomer. The values of $M_{e,\theta} = 13.3/\theta$ kg/mole have been used for the polystyrene samples.

Long polymer	θ	Z	τ_{max}	τ_c	τ_R, Eq.(8)	τ_R, Eq.(10)	T_g
PS545k	0.28	11.5	450s	0.4s	30.00s	78.27s	91.2°C
PS545k	0.525	21.5	2700s	0.25s	75.65s	133.7s	98.6°C
PS545k	0.7	28.7	10000s	0.3s	184.8s	278.3s	101.0°C
PS545k	0.9	36.9	30000s	0.3s	390.0s	505.1s	104.7°C
PS545k	1	41.0	85000s	0.6s	953.4s	1159s	106.5°C
PS910k	0.17	11.6	800s	0.7s	53.13s	135.4s	-
PS910k	0.33	22.6	6500s	0.38s	170.6s	291.9s	92.1°C

3 Interchain pressure models

For monodisperse polymer melts, Marrucci and Ianniruberto (2004) [25] introduced the idea that the tube deformation was controlled by an increase in the thermal interchain pressure (Doi and Edwards 1986) [27] with the stretch of polymers. It accurately describes the shear and extensional flows of NMMD polystyrene melts.

3.1 Dynamic tube dilation

Wagner (2014) [2] extended the interchain pressure model to entangled polymer solutions in general. The transition from melts to solutions is explained by the dynamic tube dilation idea and quantitatively controlled by the lowering of the glass transition temperatures in the solutions relative to the pure melts. The interchain pressure controls the increase in the lateral spring force. This force is based on a Rouse formulation. The evolution of the stretch, f, evaluated on a particle path at the present time, t, relative to the past time, t', is

$$\frac{\partial}{\partial t} f(t,t') = f(t,t') \frac{\partial}{\partial t} \langle \ln |\mathbf{E} \cdot \mathbf{u}| \rangle - \left(1 - \frac{2}{3} a_{_{Tg}}\right) \frac{f(t,t') - 1}{\tau_R} - \frac{2}{3} a_{_{Tg}} \frac{f(t,t')^2 \left(f(t,t')^3 - 1\right)}{3\tau_R}, \quad (6)$$

where τ_R is the Rouse time. The initial value of the stretch evolution $f(t',t') = 1$. The components of the displacement gradient tensor $\mathbf{E}$ are $E_{\mathrm{ij}}(\boldsymbol{x}, t, t') = \partial x_{\mathrm{i}} / \partial x_{\mathrm{j}}{}'$, $i = 1, 2, 3$ and $j = 1, 2, 3$ in Cartesian coordinates. (x_1', x_2', x_3') are the coordinates of a particle in the reference state at time t'. These coordinates are displaced by the coordinates (x_1, x_2, x_3) in the present state at time t. All the angular brackets represent an average, here on a unit sphere, defined as $\langle \dots \rangle = 1/(4\pi) \int_{|\mathbf{u}|=1} \dots d\mathbf{u}$.

u is a unit vector. Analytical solutions on all formulas involving unit sphere integrals can be found in Urakawa at al. (1995) [28]. a_{T_g} accounts for the change in the time-temperature shift factors due to the different glass transition temperatures of solutions and melts. Particularly for NMMD polystyrene systems, Wagner (2014) [2] defined a_{T_g} as

$$\log_{10} a_{T_g} = \frac{-c_1^0 \Delta T_g}{c_2^0 + \Delta T_g}, \tag{7}$$

based on the WLF equation (Williams et al. 1955) [29]. $\Delta T_g = T_{gm} - T_{gs}$ where T_{gm} and T_{gs} are the glass transition temperatures of the polystyrene melt and solution, respectively. For the polystyrene systems $c_1^0 = 8.99$ and $c_2^0 = 81.53$°K, with a reference temperature in the WLF equation of $T_0 = 130$°C. It is important to notice that in the present study the involved a_{T_g} values are based on the direct measurements of glass transition temperatures of the involved systems. The dependency of the glass transition temperatures on the concentration of the polystyrene solutions is shown in Figure 3.

The Rouse time τ_R in Wagner (2014) [2] is calculated as

$$\tau_R = \frac{12 M \eta_0}{\pi^2 \rho R T \theta} \left(\frac{M_{cm}}{M\theta} \right)^{2.4} \tag{8}$$

(Osaki et al. 1982; Menezes et al. 1982; Takahashi et al. 1993; Isaki et al. 2003) [30, 31, 32, 33] with M_{cm}=35 kg/mol. M is the molar mass of the long polymer and R is the gas constant. The density of the polystyrenes that we used here is ρ =1.01 g/cm^3 at the temperature of T=130°C.

To calculate the involved stresses, the stretch evolution in Equation (6) is incorporated into the molecular stress function (MSF) constitutive framework (Wagner et al. 2005) [34]. In the MSF approach the components of the stress tensor, $\sigma_{\rm ij}$, are calculated as

$$\sigma_{ij} = \int_{-\infty}^{t} M(t-t') f(t,t')^2 5 \left\langle \frac{E_{in} u_n \; E_{jm} u_m}{|\mathbf{E} \cdot \mathbf{u}|^2} \right\rangle dt'. \tag{9}$$

$M(t-t')$ is the memory function, where the BSW formulation (1) is applied here.

The a_{T_g} values in Equation (6) are well defined as they are based on the direct measured glass transition temperatures. The Rouse time is essential to the outcome of any modelling, and it has been defined in numerous ways (Menezes and Graessley 1982; Osaki et al. 2000; Osaki et al. 2001; Likhtman and McLeish 2002; Larson et al.2003) [31, 35, 36, 37, 38]. Particularly for the NMMD polystyrenes, Rasmussen and Huang (2014) [1] used a direct approach, calculating the Rouse time by the direct fitting to the measured extensional viscosity of the melts. The fittings were based on the original formulation (Wagner et al. 2005) [34] of Equation (6) for monodisperse polystyrene melts. Rasmussen and Huang (2014) [1] found the dependency of the Rouse time as

$$\tau_{max}/\tau_R = 20 \cdot (Z/21.4)^2 \tag{10}$$

where $Z = M/M_e$ is the number of entanglements and M_e =13.3 kg/mole is the entanglement molecular weight for NMMD polystyrene melts. For the oligomer dilutions a linear change with the concentration is expected for the number of entanglements, $Z = M/M_{e,\theta}$, where the entanglement molecular weight of the long polymer in the dilution is $M_{e,\theta} = M_e/\theta$. In all the following referred figures, the calculations from Wagner model (6) has been included. The dashed-dotted (- · - · -) lines are the calculations based on the Rouse time from Equation (8). The solid lines (——) are the calculations based on the Rouse time from Equation (10). The effect of adjusting the Rouse time is

the change in the onset of the strain hardening of the time dependent elongational viscosities. This defines the Rouse time into the nonlinear viscoelastic region.

The model in Equation (6) is not identical to the original model from Wagner et al. (2005) [34]. The latter one was used by Rasmussen and Huang (2014) [1] to obtain the formula for the Rouse time in Equation (10). Therefore we show the calculated startup of extensional viscosity for the 545 kg/mole NMMD polystyrene melt based on Equation (6) as a function of time in Figure 4, using both of the Rouse times. The measured extensional viscosity for the 545 kg/mole NMMD melt in the figure is taken from Huang et al. (2013a) [3]. Both Rouse times give a good prediction of the corresponding measured viscosity as expected.

To look at the transition from the melt state, we have prepared an oligomer dilution containing 90% 545 kg/mole NMMD polystyrene and the measured startup of extensional viscosity is shown in Figure 5. Due to the lowering of the entanglement number upon dilution, the deviation between the dashed-dotted and solid lines, corresponding to the two different definitions of the Rouse time, has increased. However a fine agreement with the measurements is still observed. This is also the case of the extensional viscosity of a more diluted sample containing 70% 545 kg/mole NMMD polystyrene. The measurements and the corresponding calculations are shown in Figure 6.

We have attached the extensional measurements of the 52.5% 545 kg/mole NMMD polystyrene data from Huang et al. (2013a) [3] in Figure 7. The predicted extensional viscosity, using the Rouse time in Equation (8) which is the original one used by Wagner (2014) [2], in some cases is 50% below the measurements. In comparison, the prediction using the empirically based Rouse time in Equation (10) still shows good agreement. Notice that in Wagner (2014) [2] the same calculations represented by the dashed-dotted lines were reported. The present calculations are within about 10% deviation of those calculations. This small variation is an result of the difference in the used a_{T_g} values. In our calculation, the a_{T_g} values are based on the measured glass transition temperatures of the 545 kg/mole samples, as shown in Figure 3. The difference between the calculated viscosity based on the two Rouse times is enlarged with decreasing the concentration of the 545 kg/mole polystyrene. In Figure 8, the extensional viscosity of the 28% 545 kg/mole solution is shown. Here only the calculated viscosity using the Rouse time in Equation (10) gives good agreement with the measured data.

In Figure 9 we attach the extensional viscosity of the 33% 910 kg/mole NMMD polystyrene dilution measured by Huang et al. (2015) [5]. This sample has almost the same number of entanglements as the 52.5% 545 kg/mole sample. We have here prepared a 17% 910 kg/mole NMMD polystyrene dilution containing almost the same number of entanglement number as the 28% 545 kg/mole dilution. The extensional measurements of the 17% 910 kg/mole dilution are shown in Figure 10. As observed in the 28% 545 kg/mole dilution, only calculations based on the direct fitted Rouse time using Equation (10) give good agreement with the measured data in Figure 9 and 10. This is especially the case for the most diluted samples where the the calculated extensional viscosity using the Rouse time from Equation (8) in some cases is only about 1/3 of the measured values.

3.2 Constant interchain pressure

The model by Wagner is not the only one based on interchain pressure. In the model by Rasmussen and Huang (2014) [1], which was particularly made for oligomer diluted systems, the stretch evolution was assumed to be controlled by a constant interchain pressure. It was suggested as a consequence of thermal interchain pressure from the randomly configured oligomer Kuhn chains. It was derived in Rasmussen and Huang (2014) [1] where the relation between the following formula and the basic polymer physics can be found in details.

$$\frac{df(t,t')}{dt} = f(t,t')\frac{\partial}{\partial t}\langle \ln|\mathbf{E}\cdot\mathbf{u}|\rangle - f(t,t')\frac{c(f(t,t'))\cdot f(t,t')-1}{\tau_R}. \tag{11}$$

Here the presented stretch evolution also includes the effect of the maximum extensibility of polymer chains. The maximal extensibility is represented by the number of Kuhn steps in-between entanglements, N_K/Z. $N_K = M/M_K$ is the number of Kuhn steps in the long polymer chain. For polystyrenes the molecular weight of one Kuhn step, M_K, is 0.6 kg/mol (Fang et al. 2000) [39] which is expected to be independent of concentration. In Rasmussen and Huang (2014) [1] the transition to a maximum extensibility was based on the relative Padé [40] inverse Langevin function (Ye and Sridhar 2005) [41] as

$$c(f) = \frac{(3 - f^2/\lambda^2_{max})(1 - 1/\lambda^2_{max})}{(3 - 1/\lambda^2_{max})(1 - f^2/\lambda^2_{max})}, \tag{12}$$

where $\lambda^2_{max} = N_K/Z$.

This model is in line with the classical idea that the transition to steady extensional flow should be related to the maximal extensibility of the polymer: With increasing dilution the polymer could be stretched more. The model by Wagner (2014) [2] differs. The steady state of the extensional viscosity is not linked to the maximal extensibility but a consequence of the increased thermal interchain pressure on the tube, due to the stretching of the long polymer chains. Here the transition to the steady viscosity for solutions is controlled by the value of a_{Tg}. As mentioned before, a_{Tg} is a correction factor accounting for the lowering of glass transition temperatures in solutions compared with pure melts.

For the most diluted case, the 17% 910 kg/mole NMMD polystyrene, the square of the maximal extensibility increases a factor of about 6 compared to the pure melt. Looking at the extensional viscosity in Figure 10, the dashed lines representing the constant interchain pressure model (11) capture this transition. This has similarly been observed for entangled bidisperse polystyrene systems, in the case where the short polymers were in a random state and the concentration of the large polymers was down to 4% (Rasmussen 2015) [42]. The dashed (- - -) lines in all the referred figures are the predictions using Equation (11) with the Rouse time from Equation (10). Considering the intermediate concentrations of the long polymer, i.e. the 28% 545 kg/mole, the 33% 910 kg/mole, and 52.5% 545 kg/mole NMMD polystyrenes, in Figure 8, 9, and 7 respectively, both the time dependent viscosity and the steady values are predicted accurately. For those in the transition toward the undiluted polystyrene melt, represented by the measurements of the extensional viscosity of the 70% 545 kg/mole and 90% 545 kg/mole NMMD polystyrenes in Figure 6 and 5 respectively, agreement between the constant interchain pressure model (11) and the measured data is still observed, but not as good as the lower concentrations. Finally, by comparing the model with the extensional viscosity of the undiluted 545 kg/mole sample, it is clear that Equation (11) is unable to predict the flow dynamics of NMMD polystyrene melts.

4 Discussion and conclusion

We have here performed extensional measurements on oligomer diluted NMMD polystyrene solutions at a wide range of concentration from 90% down to 17%, and also looked into the transition from the pure melt state to the diluted state. We have shown agreement between the measurements and the model by Wagner (2014) [2] using the Rouse time as calculated in Rasmussen and Huang (2014) [1]. Further, in all the diluted cases a constant interchain pressure assumption with maximum extensibility controlled by the number of Kuhn steps in-between entanglements (Rasmussen and Huang 2014) [1] also shows agreement with the measured data.

Considering extensional viscosities of monodisperse melts the model by Wagner (2014), based on the dynamic tube dilation idea, has not been applied to other systems than polystyrene yet. Masubuchi et al. (2014) [13] theoretically looked into the extensional viscosities some of monodisperse melts considering monomeric friction reduction. Their model (Masubuchi et al. 2014) [13] was able

to predict the (steady) extensional viscosity of the polyisoprene from Sridhar et al. (2014) [45] within the same framework as for the polystyrenes, whereas it was not possible to capture the behaviour of the NMMD poly(n-butyl acrylate) melt (Sridhar et al. 2014) [45]). However, the constant interchain pressure model (Rasmussen and Huang 2014 [1]), which was never intended for NMMD melts, was surprisingly able to predict the extensional viscosity of the NMMD polyisoprenes (Rasmussen 2016) [47] measured by Nielsen et al. (2009) [43] and Liu et al. (2013) [44] and also the NMMD poly(n-butyl acrylate) melt [48] measured in extension by Sridhar et al. (2014) [45].

Acknowledgement

QH would like to acknowledge financial support from the Aage og Johanne Louis–Hansen Foundation.

References

[1] Rasmussen HK, Huang Q (2014) Interchain tube pressure effect in extensional flows of oligomer diluted nearly monodisperse polystyrene melts. Rheologica Acta 53(3):199-208

[2] Wagner MH (2014) Scaling relations for elongational flow of polystyrene melts and concentrated solutions of polystyrene in oligomeric styrene. Rheologica Acta 53(10):765-777

[3] Huang Q, Mednova O, Rasmussen HK, Alvarez HJ, Skov AL, Almdal K, Hassager O (2013a) Concentrated polymer solutions are different from melts: Role of entanglement molecular weight. Macromolecules 46(12):5026-5035

[4] Huang Q, Alvarez NJ, Matsumiya Y, Rasmussen HK, Watanabe H, Hassager O (2013b) extensional rheology of entangled polystyrene solutions suggests importance of nematic interactions. ACS Macro Letters 2(8):741-744

[5] Huang Q, Hengeller L, Alvarez NJ, Hassager O (2015) Bridging the gap between polymer melts and solutions in extensional rheology. Macromolecules 48(12):4158-4163

[6] Wingstrand SL, Alvarez NJ, Huang Q, Hassager O (2015) Linear and nonlinear universality in the rheology of polymer melts and solutions. Physical review letters 115(7):078302

[7] Bhattacharjee PK, Oberhauser JP, McKinley GH, Leal GL, Sridhar T (2002) Extensional rheometry of entangled solutions. Macromolecules 35(27):10131-10148

[8] Bach A, Almdal K, Rasmussen HK, Hassager O (2003b) Elongational viscosity of narrow molar mass distribution polystyrene. Macromolecules 36(14):5174-5179

[9] Rasmussen HK, Huang Q (2014) The missing link between the extensional dynamics of polymer melts and solutions. Journal of Non-Newtonian Fluid Mechanics 204:1-6

[10] Vinogradov GV, Malkin AY, Volosevitch VV, Shatalov VP, Yudin VP (1975) Flow, high-elastic (recoverable) deformation, and rupture of uncured high molecular weight linear polymers in uniaxial extension. Journal of Polymer Science: Polymer Physics Edition 13(9):1721-1735

[11] Yaoita T, Isaki T, Masubuchi Y, Watanabe H, Ianniruberto G, Marrucci G (2012) Primitive Chain Network Simulation of Elongational Flows of Entangled Linear Chains: Stretch/Orientation-induced Reduction of Monomeric Friction. Macromolecules 45(6):2773-2782

[12] Ianniruberto G, Brasiello A, Marrucci G (2012) Simulations of fast shear flows of PS oligomers confirm monomeric friction reduction in fast elongational flows of monodisperse PS melts as indicated by rheooptical data. Macromolecules 45(19):8058-8066

[13] Masubuchi Y, Matsumiya Y, Watanabe H (2014) Test of Orientation/Stretch-Induced Reduction of Friction via Primitive Chain Network Simulations for Polystyrene, Polyisoprene, and Poly(n.butyl acrylate). Macromolecules 47(19):6768-6775

[14] Ianniruberto G (2015) Extensional flows of solutions of entangled polymers confirm reduction of friction coefficient. Macromolecules 48(17):6306-6312

[15] Park GW, Ianniruberto G (2017), Flow-Induced Nematic Interaction and Friction Reduction Successfully Describe PS Melt and Solution Data in Extension Startup and Relaxation. Macromolecules, DOI: 10.1021/acs.macromol.7b00208

[16] Sridhar T, Acharya M, Nguyen D, Bhattacharjee PK (2014) On the Extensional Rheology of Polymer Melts and Concentrated Solutions. Macromolecules 47(1):379-386

[17] Baumgaertel M, Winter HH (1992) Interrelation between continuous and discrete relaxation time spectra. Journal of Non-Newtonian Fluid Mechanics 44(1):15-36

[18] Baumgaertel M, Schausberger A, Winter HH (1990) The relaxation of polymers with linear flexible chains of uniform length. Rheologica Acta 29(5):400-408

[19] Rasmussen HK, Christensen JH, Gøttsche SJ (2000) Inflation of polymer melts into elliptic and circular cylinders. Journal of Non-Newtonian Fluid Mechanics 93(2-3):245-263

[20] Bach A, Rasmussen HK, Hassager O (2003a) Extensional viscosity for polymer melts measured in the filament stretching rheometer. Journal of Rheology 47(2), 429-441

[21] Marin JMR, Huusom JK, Alvarez NJ, Huang Q, Rasmussen HK, Bach A, Skov AL, Hassager O (2013) A control scheme for filament stretching rheometers with application to polymer melts. Journal of Non-Newtonian Fluid Mechanics 194:14-22

[22] Rasmussen HK, Bejenariu AG, Hassager O, Auhl D (2010) Experimental evaluation of the pure configurational stress assumption in the flow dynamics of entangled polymer melts. Journal of Rheology 54(6):1325-1336

[23] Szabo P (1997) Transient filament stretching rheometer part I: Force Balance analysis. Rheologica Acta 36(3):277-284

[24] Nielsen JK, Rasmussen HK, Hassager O (2008) Stress relaxation of narrow molar mass distribution polystyrene following uni-axial extension. Journal of Rheology 52(4):885-899

[25] Marrucci G, Ianniruberto G (2004) Interchain pressure effect in extensional flows of entangled polymer melts. Macromolecules 37():3934-3942

[26] Rasmussen HK, Huang Q (2017) Constant interchain pressure effect in extensional flows of oligomer diluted polystyrene and poly(methyl methacrylate) melts. Rheologica Acta 56(1):27-34

[27] Doi M, Edwards SF (1986) The Theory of Polymer Dynamics. Clarendon Press: Oxford

[28] Urakawa O, Takahashi M, Masuda T, Golshan Ebrahimi N (1995) Damping functions and chain relaxation in uniaxial and biaxial extensions: Comparison with the Doi-Edwards theory. Macromolecules 28(21):7196-7201

[29] Williams ML, Landel RF, Ferry JD (1955) The temperature dependence of relaxation mechanisms in amorphous polymers and other glass-forming liquids. Journal of the American Chemical Society 77(14):3701-3707

[30] Osaki K, Nishizawa K, Kurata M (1982) Material time constant characterizing the nonlinear viscoelasticity of entangled polymeric systems. Macromolecules 15(4):1068-1071

[31] Menezes EV, Graessley WW (1982) Nonlinear rheological behavior of polymer systems for several shear-flow histories. Journal of Polymer Science part B - Polymer Physics 20(10):1817-1833

[32] Takahashi M, Isaki T, Takigawa T, Masuda T (1993) Measurement of biaxial and uniaxial extensional flow behavior of polymer melts at constant strain rates. Journal of Rheology 37(5):827-846

[33] Isaki T, Takahashi M, Urakawa O (2003) Biaxial damping function of entangled monodisperse polystyrene melts: Comparison with the Mead-Larson-Doi model. Journal of Rheology 47(5):1201-1210

[34] Wagner MH, Kheirandish S , Hassager O (2005) Quantitative prediction of transient and steady-state elongational viscosity of nearly monodisperse polystyrene melts. Journal of Rheology 49(6):1317-1327

[35] Osaki K, Inoue T, Isomura T (2000) Stress Overshoot of Polymer Solutions at High Rates of Shear. Journal of Polymer Science part B - Polymer Physics 38(14):1917-1925

[36] Osaki K, Inoue T , Uematsu T, Yamashita Y (2001) Evaluation methods of the longest Rouse relaxation time of an entangled polymer in a semidilute solution. Journal of Polymer Science part B - Polymer Physics 39(14):1704-1712

[37] Likhtman AE, McLeish TCB (2002) Quantitative Theory for Linear Dynamics of Linear Entangled Polymers, Macromolecules 35(16):6332-6343.

[38] Larson RG, Sridhar T, Leal LG, McKinley GH, Likhtman AE, McLeish TCB (2003) Definitions of entanglement spacing and time constants in the tube model. Journal of Rheology 47(3):809-818

[39] Fang J, Kröger M, Öttinger HC (2000) A thermodynamically admissible reptation model for fast flows of entangled polymers. II. Model predictions for shear and extensional flows. Journal of Rheology 44(6):1293-1317

[40] Cohen A (1991) A Padé approximant to the inverse Langevin function. Rheologica Acta 30(3):270-273

[41] Ye X, Sridhar T (2005) Effects of the polydispersity on rheological properties of entangled polystyrene solutions. Macromolecules 38(8):3442-3449

[42] Rasmussen HK (2015) Interchain tube pressure effect in the flow dynamics of bi-disperse polymer melts. Rheologica Acta 54(1):9-18

[43] Nielsen JK, Hassager O, Rasmussen HK, McKinley GH (2009) Observing the chain stretch transition in a highly entangled polyisoprene melt using transient extensional rheometry. Journal of Rheology 53(6):1327-1346

[44] Liu G, Sun H, Rangou S, Ntetsikas K, Avgeropoulos A, Wang S-Q (2013) Studying the origin of "strain hardening": Basic difference between extension and shear. Journal of Rheology 57(1):89-104

[45] Sridhar T, Acharya M, Nguyen DA, Bhattacharjee PK (2014) On the Extensional Rheology of Polymer Melts and Concentrated Solutions. Macromolecules, 47(1):379-386

[46] Alvarez N (2016) Effect of Chain Flexibility on Non-linear Extensional Response of Linear Polymer Melts. The XVIIth International Congress on Rheology 5562

[47] Rasmussen HK (2016) A constitutive analysis of the extensional flows of nearly monodisperse polyisoprene melts. Polymer 104():251-257

[48] Rasmussen HK, Huang Q (2016) Constant interchain tube pressure effect on flow of monodisperse polymer melts and oligomer dilutions. The XVIIth International Congress on Rheology

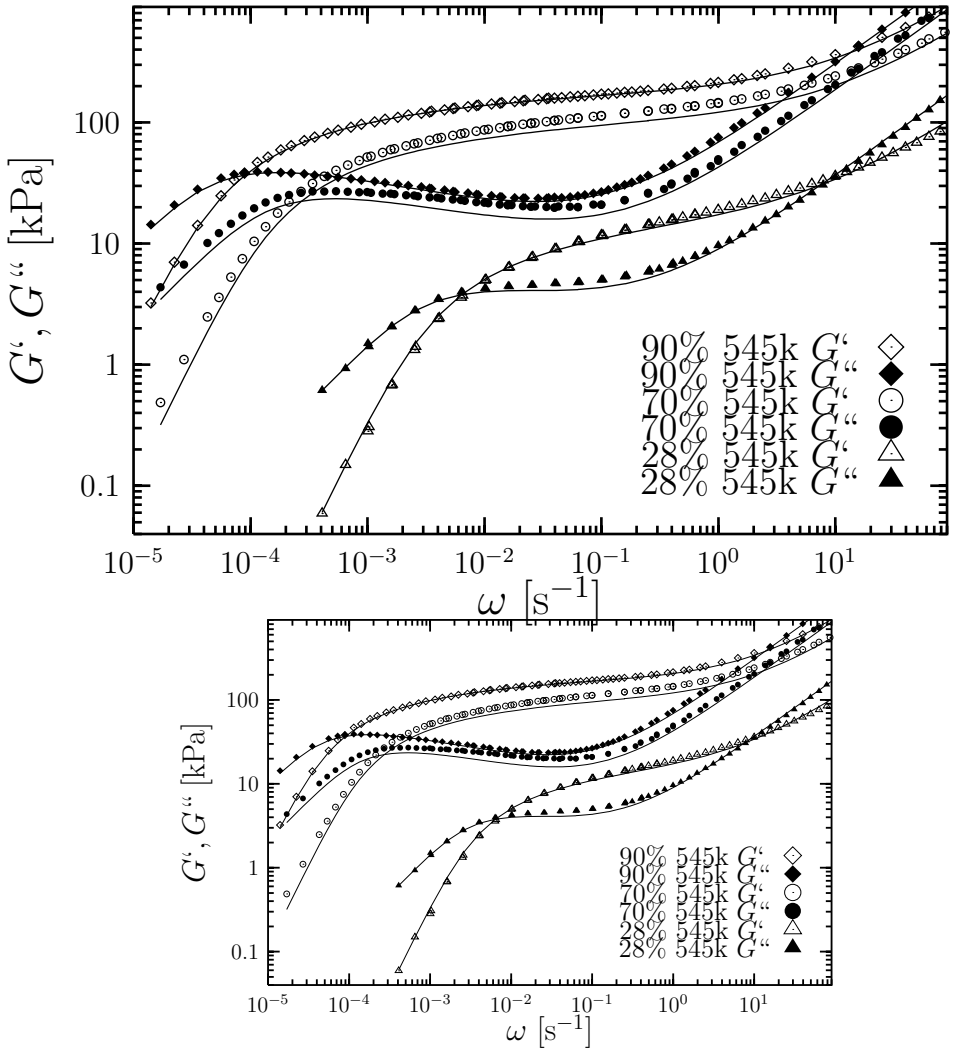

Figure 1: Loss, G'' (filled symbols) and storage moduli, G' (open symbols), both as a function of the angular frequency ω measured at 130°C for a 545 kg/mole NMMD polystyrene, diluted in the 4.29 kg/mole styrene oligomer. The top to the bottom data are a 90% (box), a 70% (circle) and a 28% (triangles) 545 kg/mole dilution. The solid lines (——) are the least-square fittings to the BSW model in Equation (2).

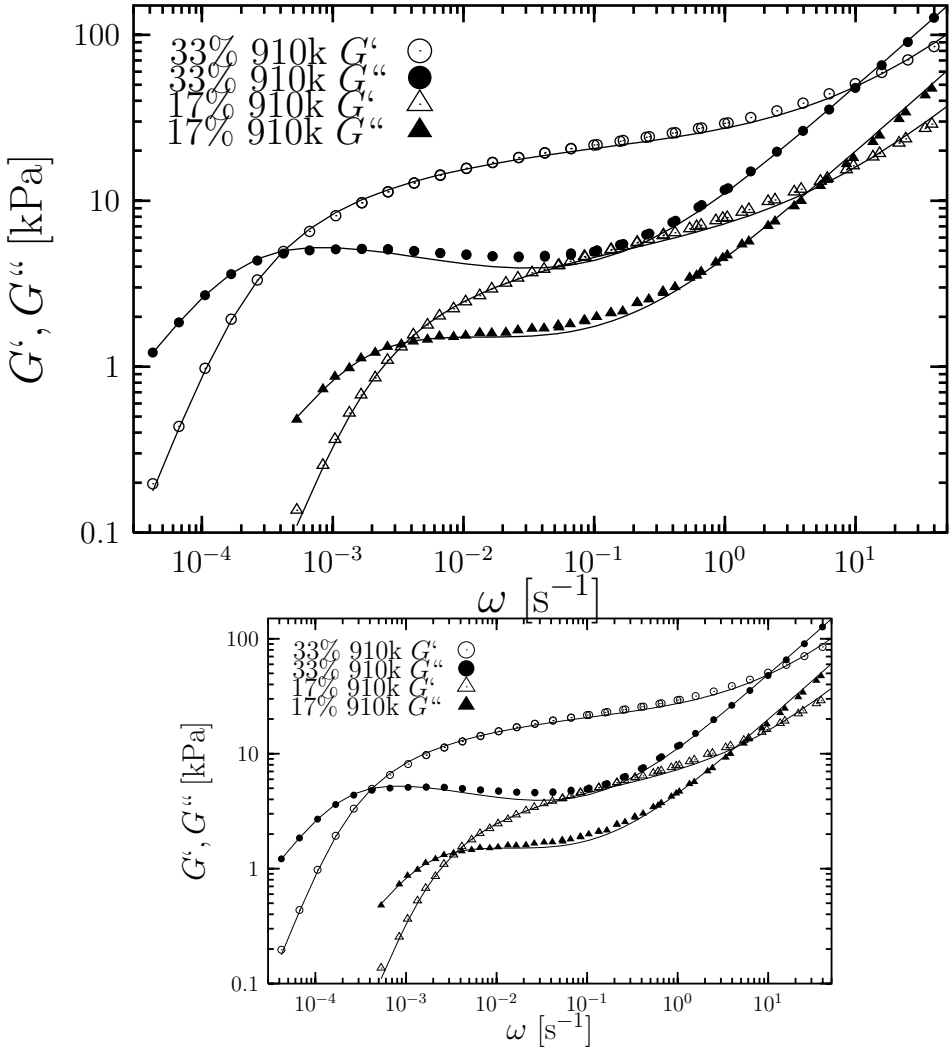

Figure 2: Loss, G'' (filled symbols) and storage moduli, G' (open symbols), both as a function of the angular frequency ω measured at 130°C for a 910 kg/mole NMMD polystyrene, diluted in the 4.29 kg/mole styrene oligomer. The top to the bottom data are a 33% (circle) and a 17% (triangles) 910 kg/mole dilution. The measured data of the 33% dilution originates from Huang et al. (2015) [5], measured at 130°C. The solid lines (——) are the least-square fittings to the BSW model in Equation (1).

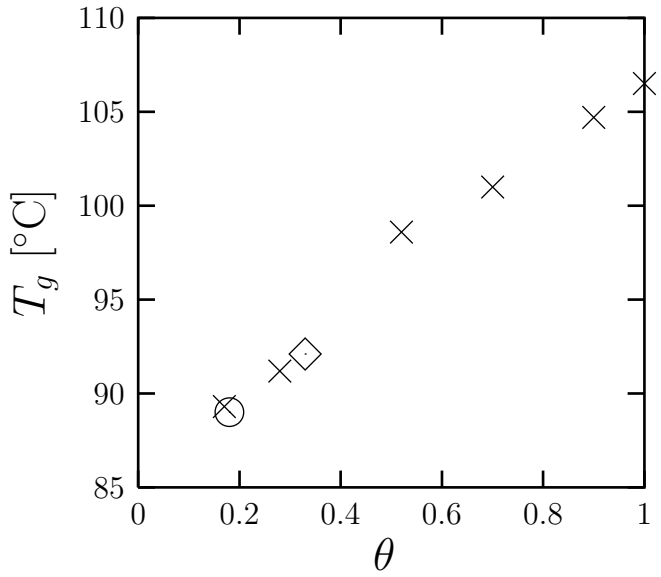

Figure 3: Glass transition temperatures of polystyrene diluted in 4.29 kg/mole styrene oligomer as a function of the weight fraction, θ, of the long polymer in the oligomer. The crosses ($\times$) are all dilutions with the 545 kg/mole NMMD polystyrene as the large polymer, whereas the diamond ($\diamond$) is the 910 kg/mole NMMD polystyrene dilution from Huang et al. (2015) [5] and the circle ($\circ$) the 1760 kg/mole NMMD polystyrene dilution from Huang et al. (2015) [5].

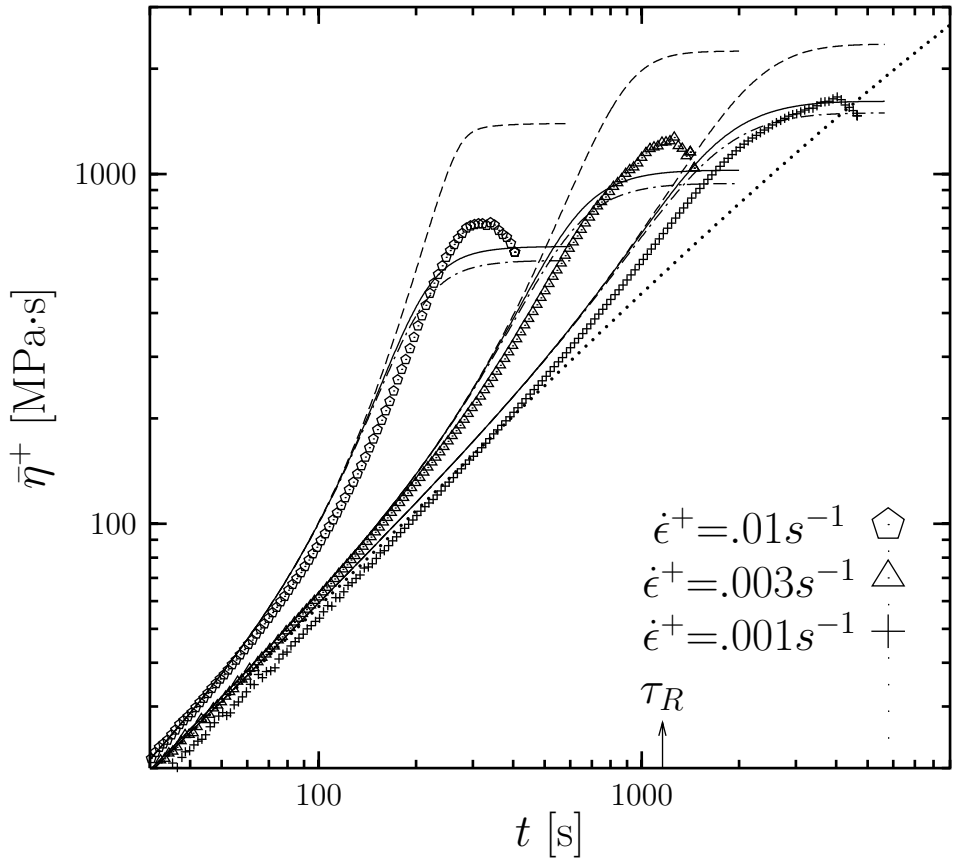

Figure 4: The startup of extensional viscosity, $\bar{\eta}^+$, as a function of time at 130°C. The symbols are the measurements of a 545 kg/mole NMMD polystyrene melt. These data originates from Huang et al. (2013) [3]. The dashed-dotted (- · - · -) and solid lines (——) and are the corresponding predictions to the data from Equation (6) using the Rouse time in Equation (8) and (10) respectively. The dashed lines (- - -) are the corresponding predictions to the data from Equation (11). The dotted line (· · ·) is the linear viscoelastic predictions based on the parameters listed in Table 1 using Equation (2).

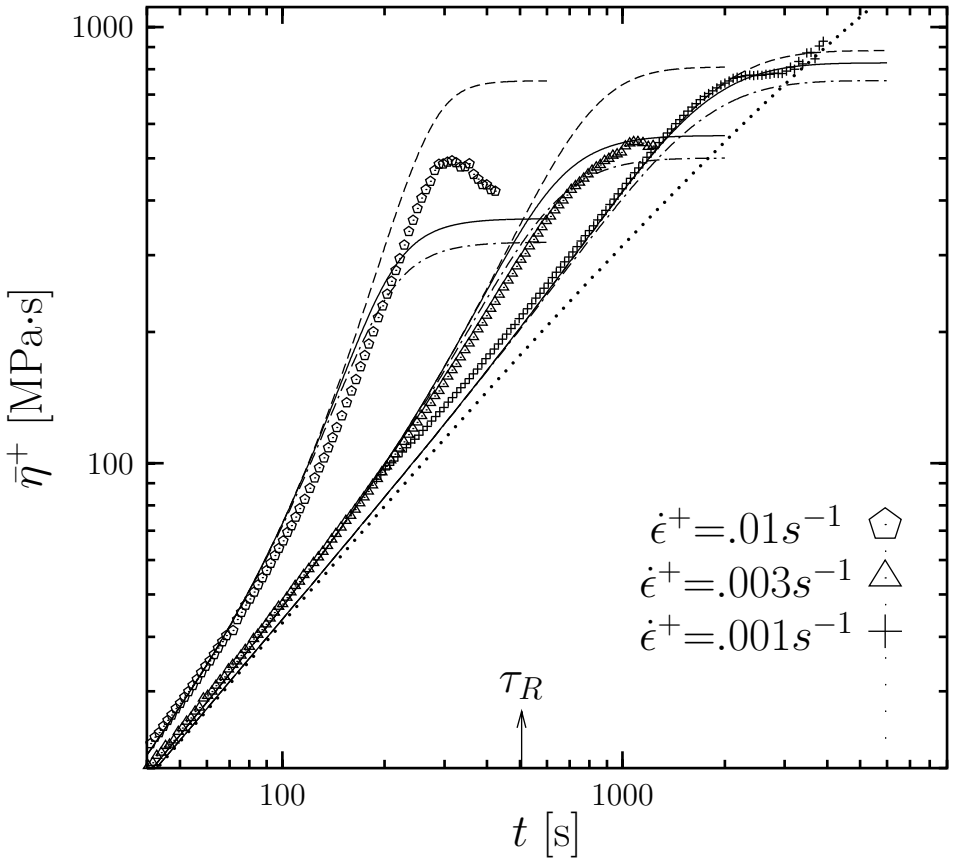

Figure 5: The startup of extensional viscosity, $\bar{\eta}^+$, as a function of time at 130°C. The symbols are the measurements of a 90%($\theta = 0.90$) 545 kg/mole NMMD polystyrene diluted in the 4.29 kg/mole oligomer. The dashed-dotted (- · - · -) and solid lines (——) and are the corresponding predictions to the data from Equation (6) using the Rouse time in Equation (8) and (10) respectively. The dashed lines (- - -) are the corresponding predictions to the data from Equation (11). The dotted line (· · ·) is the linear viscoelastic predictions based on the parameters listed in Table 1 using Equation (2).

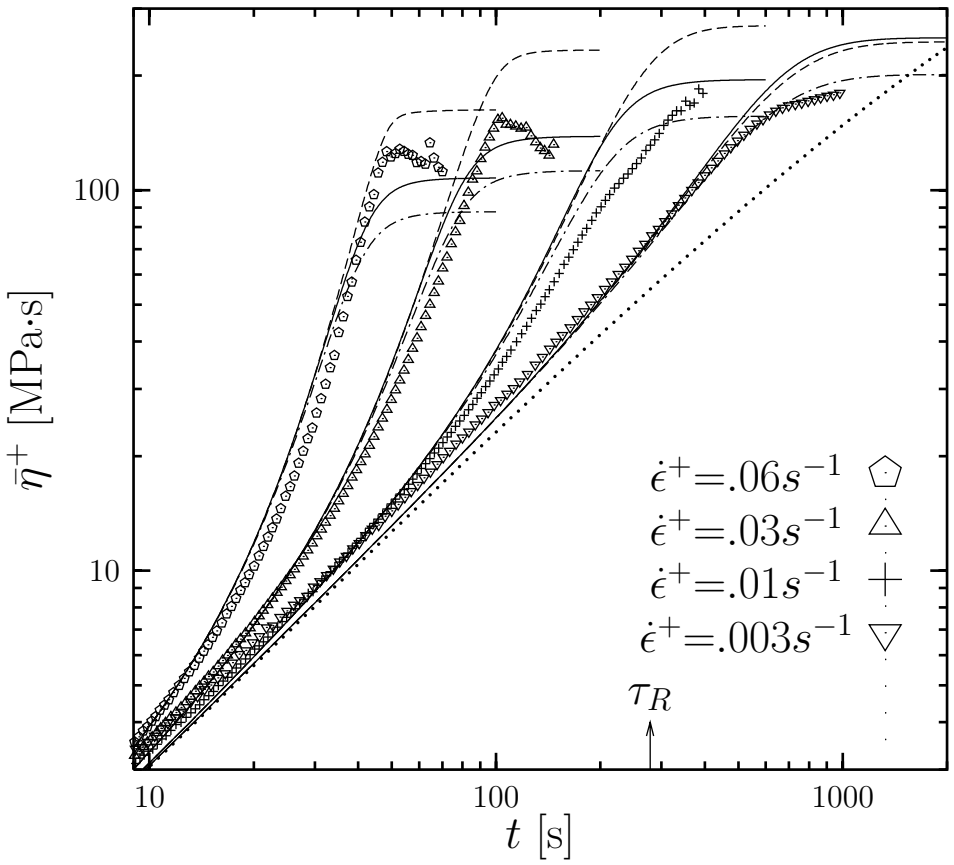

Figure 6: The startup of extensional viscosity, $\bar{\eta}^+$, as a function of time at 130°C. The symbols are the measurements of a 70%($\theta = 0.70$) 545 kg/mole NMMD polystyrene diluted in the 4.29 kg/mole oligomer. The dashed-dotted (- · - · -) and solid lines (——) and are the corresponding predictions to the data from Equation (6) using the Rouse time in Equation (8) and (10) respectively. The dashed lines (- - -) are the corresponding predictions to the data from Equation (11). The dotted line (· · ·) is the linear viscoelastic predictions based on the parameters listed in Table 1 using Equation (2).

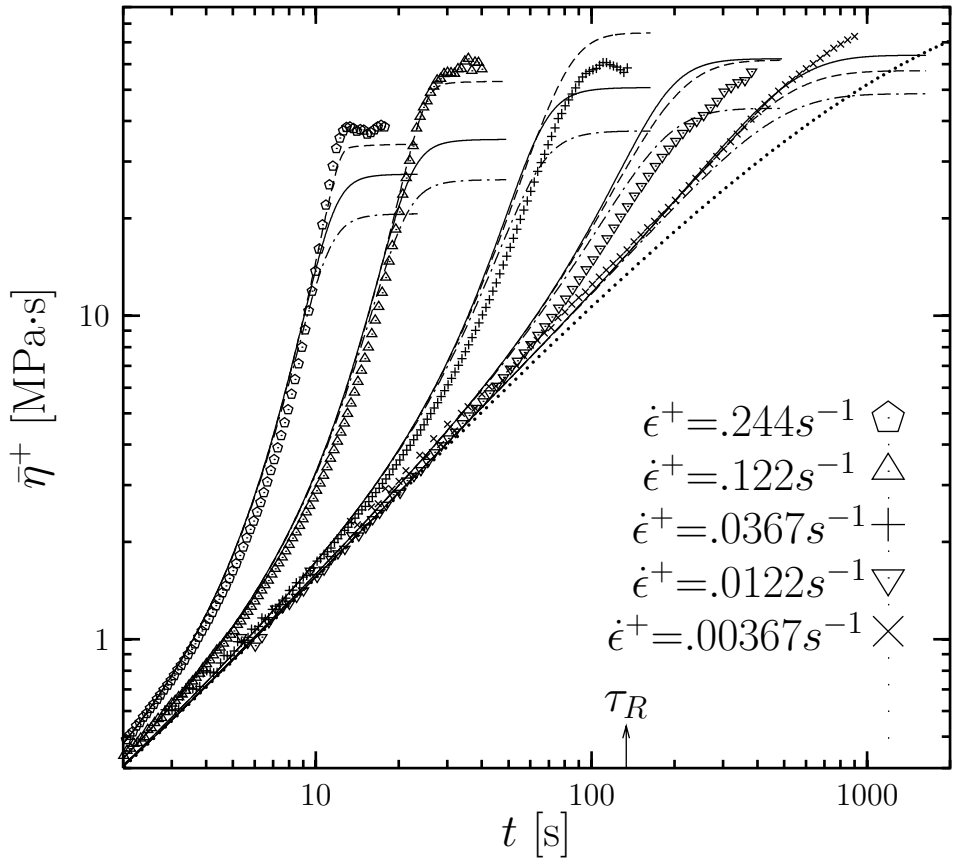

Figure 7: The startup of extensional viscosity, $\bar{\eta}^+$, as a function of time at 130°C. The symbols are the measurements of a 52.5%($\theta = 0.525$) 545 kg/mole NMMD polystyrene diluted in the 4.29 kg/mole oligomer. These data originates from Huang et al. (2013) [3], measured at 129°C, here time-temperature superposition shifted to 130°C. The dashed-dotted (- · - · -) and solid lines (——) and are the corresponding predictions to the data from Equation (6) using the Rouse time in Equation (8) and (10) respectively. The dashed lines (- - -) are the corresponding predictions to the data from Equation (11). The dotted line ($\cdots$) is the linear viscoelastic predictions based on the parameters listed in Table 1 using Equation (2).

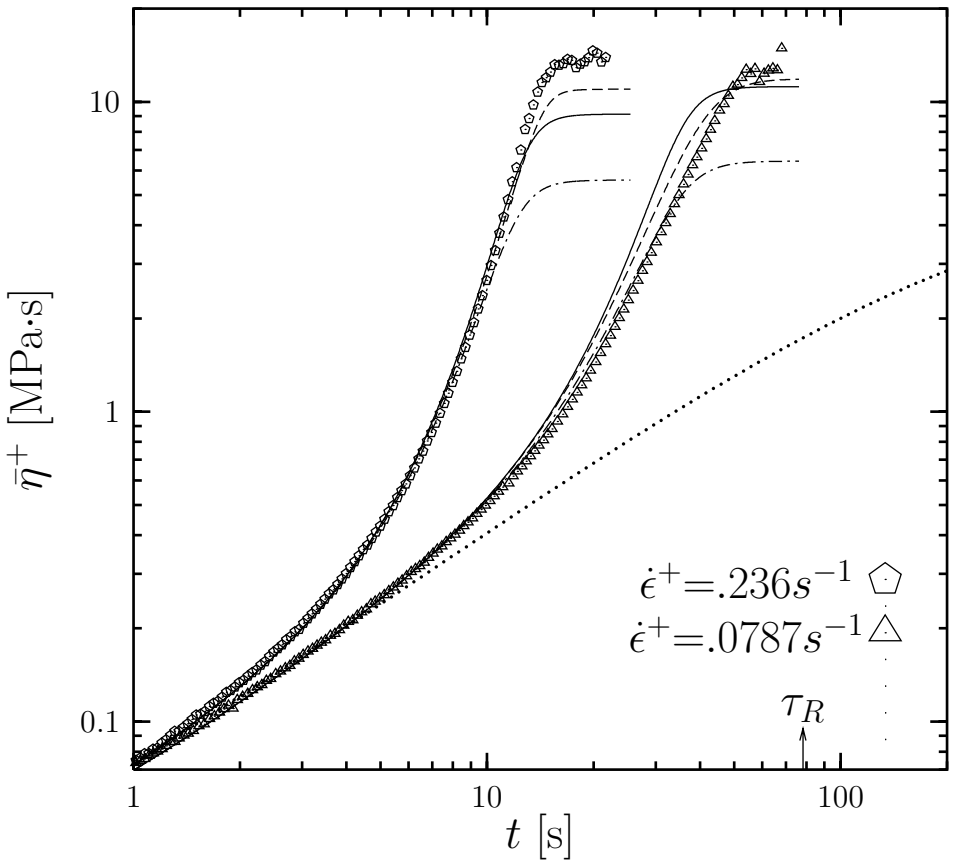

Figure 8: The startup of extensional viscosity, $\bar{\eta}^+$, as a function of time at 130°C. The symbols are the measurements of a 28%($\theta = 0.28$) 545 kg/mole NMMD polystyrene diluted in the 4.29 kg/mole oligomer. The dashed-dotted (- · - · -) and solid lines (——) and are the corresponding predictions to the data from Equation (6) using the Rouse time in Equation (8) and (10) respectively. The dashed lines (- - -) are the corresponding predictions to the data from Equation (11). The dotted line (· · ·) is the linear viscoelastic predictions based on the parameters listed in Table 1 using Equation (2).

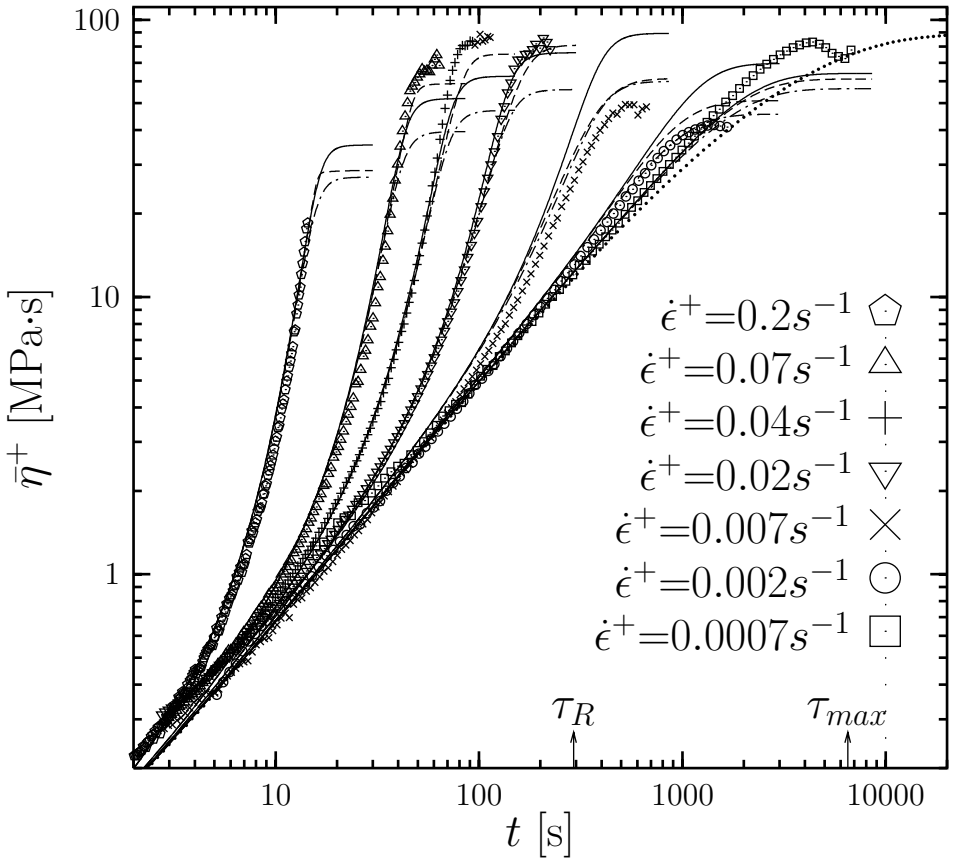

Figure 9: The startup of extensional viscosity, $\bar{\eta}^+$, as a function of time at 130°C. The symbols are the measurements of a 33%($\theta = 0.33$) 910 kg/mole NMMD polystyrene diluted in the 4.29 kg/mole oligomer. These data originates from Huang et al. (2015) [5]. The dashed-dotted (- · - · -) and solid lines (——) and are the corresponding predictions to the data from Equation (6) using the Rouse time in Equation (8) and (10) respectively. The dashed lines (- - -) are the corresponding predictions to the data from Equation (11). The dotted line (· · ·) is the linear viscoelastic predictions based on the parameters listed in Table 1 using Equation (2).

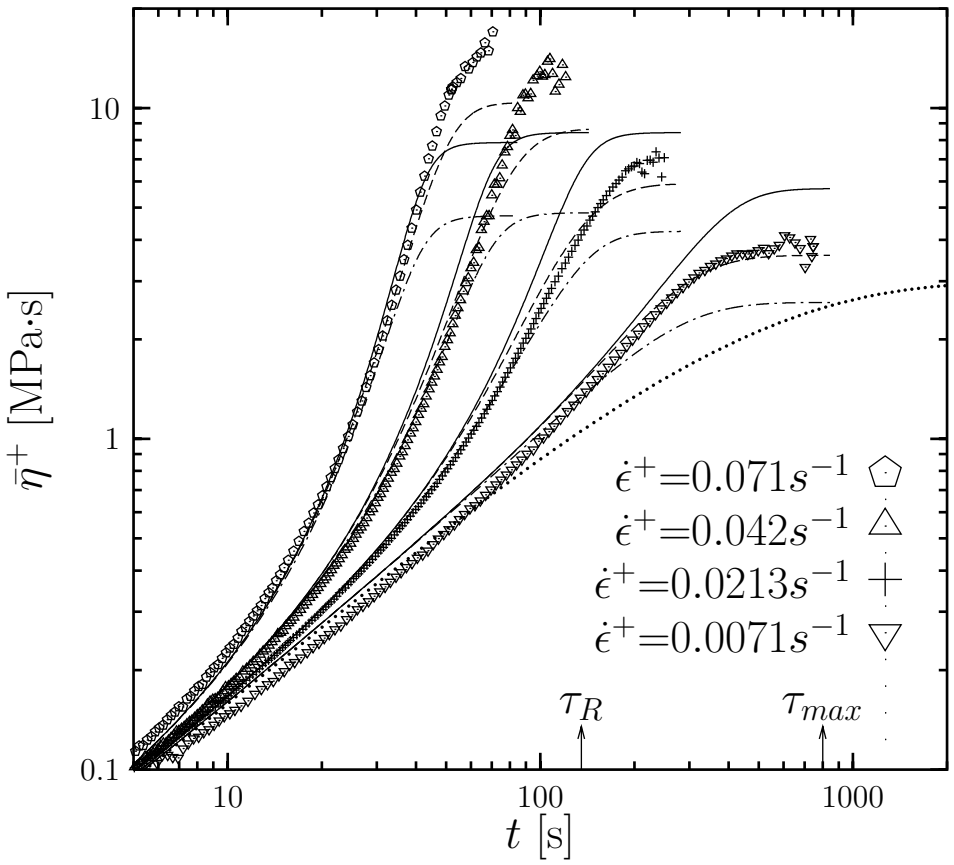

Figure 10: The startup of extensional viscosity, $\bar{\eta}^+$, as a function of time at 130°C. The symbols are the measurements of a 17%($\theta = 0.17$) 910 kg/mole NMMD polystyrene diluted in the 4.29 kg/mole oligomer. The dashed-dotted (- · - · -) and solid lines (——) and are the corresponding predictions to the data from Equation (6) using the Rouse time in Equation (8) and (10) respectively. The dashed lines (- - -) are the corresponding predictions to the data from Equation (11). The dotted line (· · ·) is the linear viscoelastic predictions based on the parameters listed in Table 1 using Equation (2).